PHOTO-FERMENTATIVE HYDROGEN PRODUCTION FROM ORGANIC ACIDS MIXTURES EVALUATED THROUGH PREDICTIVE MODELS FOR Rhodobacter capsulatus STRAINS

Santiago Rodríguez-Valderrama, Carlos Escamilla-Alvarado, Jean-Pierre Magnin, Pasiano Rivas-García, Héctor Javie Amézquita-García, José Julián Cano-Gómez

HAL Id: hal-03723677

https://hal.univ-grenoble-alpes.fr/hal-03723677v1

Submitted on 15 Jul 2022

PHOTO-FERMENTATIVE HYDROGEN PRODUCTION FROM ORGANIC ACIDS MIXTURES EVALUATED THROUGH PREDICTIVE MODELS FOR *Rhodobacter capsulatus* STRAINS

Producción fotofermentativa de hidrógeno a partir de mezclas de ácidos orgánicos evaluada mediante modelos predictivos para cepas de *Rhodobacter capsulatus*

Santiago RODRÍGUEZ-VALDERRAMA[1,2], Carlos ESCAMILLA-ALVARADO[1]*, Jean-Pierre MAGNIN[2], Pasiano RIVAS-GARCÍA[1], Héctor Javier AMÉZQUITA-GARCÍA and José Julián CANO-GÓMEZ[1]

[1] Centro de Investigación en Biotecnología y Nanotecnología, Facultad de Ciencias Químicas, Grupo de Ingeniería y Bioprocesos Sustentables, Universidad Autónoma de Nuevo León, km 10 Highway to International Airport Mariano Escobedo, 66629, Apodaca, Nuevo León, Mexico.

[2] Laboratoire de Electrochimie et physico-chimie des matériaux et des interfaces, Institute d'ingénierie et de management, Université de Grenoble Alpes 38000 Grenoble, France.

*Author for correspondence: cea_escamilla@yahoo.com.mx

ABSTRACT

This research aimed to evaluate growth and hydrogen production from *Rhodobacter capsulatus* DSM155 and B10 strains in function of volatile fatty acids (VFA) media composition, as well as to assess the light intensity effect on hydrogen production. The growth of DSM155 and B10 was verified in media containing either acetic acid, butyric acid, or sodium lactate, or a mixture of them (ABL medium), being the ABL medium that produced the maximum cell dry weight, 2.15 and 1.67 g/L for DSM155 and B10, respectively. Biohydrogen production was evaluated in media containing acetic and butyric acids (AB medium), and ABL medium. Both strains presented the highest hydrogen production using ABL medium, being the highest 239.2 mL H_2 for DSM155. Finally, light intensity (10, 20, and 30 klux) effect on biohydrogen production was studied using the best strain and medium, i.e., DSM155 and ABL medium. DSM155 produced hydrogen increasingly in the order 10, 20, and 30 klx (2753.5, 2850.5, and 2946.3 mL H_2/L_{op}, respectively); however, the light conversion efficiency into hydrogen showed an inverse trend, 7.47, 4.16, and 2.67 %. In conclusion, *R. capsulatus* DSM155 is advisable for biohydrogen production using ABL medium in the range 10-30 klux. Moreover, further work is recommended on DSM 155 using organic acid-rich real effluents from dark fermentation.

RESUMEN

El objetivo de esta investigación fue evaluar el crecimiento y la producción de hidrógeno de las cepas *Rhodobacter capsulatus* DSM155 y B10 en función de la composición del medio con ácidos grasos volátiles (AGV), así como evaluar el efecto de la intensidad de la luz en la producción de hidrógeno. El crecimiento de las cepas DSM155 y B10 se verificó en medios que contenían ácido acético, ácido butírico o lactato de sodio, o una mezcla de ellos (medio ABL), siendo el medio ABL el que produjo el máximo peso seco celular, 2.15 y 1.67 g/L para DSM155 y B10, respectivamente. La producción de biohidrógeno se evaluó en medios que contenían ácido acético y butírico (medio AB), y en el medio ABL. Ambas cepas presentaron la mayor producción de hidrógeno utilizando el medio ABL, siendo la más alta de 239.2 mL H_2 para DSM155. Por último, se estudió el efecto de la intensidad de la luz (10, 20 y 30 klux) sobre la producción de biohidrógeno utilizando la mejor cepa y el mejor medio, es decir, DSM155 y el medio ABL. DSM155 produjo hidrógeno de forma creciente en el orden de 10, 20 y 30 klx (2753.5, 2850.5 y 2946.3 mL H_2/L_{op}, respectivamente); sin embargo, la eficiencia de conversión de luz en hidrógeno mostró una tendencia inversa, 7.47, 4.16 y 2.67 %. En conclusión, *R. capsulatus* DSM155 es recomendable para la producción de biohidrógeno utilizando el medio ABL en el rango de 10-30 klux. Además, se recomienda seguir trabajando con DSM155 utilizando efluentes reales ricos en ácidos orgánicos procedentes de la fermentación oscura.

INTRODUCTION

Hydrogen is considered as a clean fuel (absolute carbon-zero nature) and an efficient energy carrier (lower to higher heating values of 122-142 kJ/g). Nowadays, hydrogen is principally produced from fossil resources (natural gas, coal, and oil) by different physical-chemical processes, which greenhouse gas emissions, high energy input requirements, and non-renewable sources depletion are the main disadvantages (Ghosh et al. 2017). Alternatively, hydrogen can be produced via biological processes (bio-photolytic and fermentative processes). These biological hydrogen (biohydrogen) production pathways are considered green technologies due to beneficial traits such as low operational requirements (i.e., low pressures and near ambient temperatures), organic wastes valorization, and low carbon emissions, among others (Rodríguez-Valderrama et al. 2019, Tiang et al. 2020).

The biohydrogen production processes can be classified into light-dependent and non-light-dependent processes. The former classification includes bio-photolysis carried out by microalgae and cyanobacteria, and photofermentation driven by photofermentative (PF) bacteria. Dark fermentation (DF) is the sole non-light-dependent biohydrogen process still known (Argun and Kargi 2011). Biohydrogen production by PF is renowned for its high biohydrogen yields, ample spectrum of light use, and profiting from different carbon sources such as carbohydrates and volatile fatty acids (VFA) (Keskin et al. 2011).

PF is mainly carried out by purple non-sulfur bacteria (PNSB) such as *Rhodobacter sphaeroïdes*, *R. capsulatus*, *Rhodovulum sulfidophilum*, and *Rhodopseudomonas palustris*, requiring anoxygenic conditions for effective biohydrogen production (Ghosh et al. 2017). PNSB may produce hydrogen from pure substances such as simple sugars (e.g., glucose, fructose, sucrose) or organic acids (malic acid, lactic acid, acetic acid, propionic acid, butyric acid), and complex carbon sources (e.g., sugar refinery wastewater, brewery wastewater, and DF effluents) (Magnin and Deseure 2019). Complex carbon sources may require a pre-adaptation in order to be successfully transformed into hydrogen. For instance, DF effluents rich in organic acids can be used as substrate for PNSB to produce hydrogen; nevertheless, different compounds in DF effluents can limit the PF performance (e.g., ammonium ion, furfural, phenolic compounds, color, and multiple carbon sources). For the first three, dilution strategies, activated carbon detoxification treatments have been applied, while the presence of multiple carbon sources (e.g., sugars, volatile fatty acids, lipids) becomes a bottleneck as some carbon sources may not be effectively metabolized. In this sense, a pre-adaptation of the PNSB to media containing carbon sources similar to those in the DF effluents could improve the photofermentation performance (Lazaro et al. 2015, Tiang et al. 2020).

Other factors besides carbon source affecting the hydrogen production by PNSB are strain type, initial carbon source concentration, initial cell concentration, temperature, initial pH, light source type, carbon to nitrogen (C/N) ratio, and light intensity, being the last two the most important studied in the literature (Shi and Yu 2005). On the other hand, the optimum light intensity varies between different species and between the same species' strains and is mainly due to photo-adaptation processes. However, each strain has a minimum threshold of light intensity to initiate growth and hydrogen production as well as a saturation value in which the enzyme nitrogenase loses the ability to process excess ATP (Lazaro et al. 2015).

Kinetic parameters are a starting point to design and operate bioreactors and describe the hydrogen production progress, substrate consumption, bacterial growth, secondary metabolites formation, among others (Mu et al. 2007, Wang and Wan 2009). The modified Gompertz model has been widely used to describe hydrogen production and to estimate maximum cumulative hydrogen production in both light-dependent and non-light-dependent processes (Rodríguez-Valderrama et al. 2020a, Wang and Wan 2009). Some Gompertz model re-parametrizations have been found in the literature because they allow accessible parameter interpretation (Tjørve and Tjørve 2017). Another less commonly used sigmoidal model for predicting cumulative hydrogen production is the Boltzmann sigmoidal model, which is characterized by its ability to predict hydrogen production behavior from the lag phase to the stationary phase (Carlozzi 2009). Comparing such different models allows a better characterization of the parameters influencing most hydrogen production systems (Tjørve and Tjørve 2017).

In this study, biohydrogen production by photosynthetic bacteria *Rhodobacter capsulatus* DSM155 and *R. capsulatus* B10 was evaluated through the following set of experiments: *i)* growth assays on single-VFA and ABL, *ii)* hydrogen production by DSM155 and B10 in AB medium and ABL medium, and *iii)* light intensity effect experiments on biohydrogen production and the comparison between the different fitting models using the best strain and medium from the previous experiment.

MATERIALS AND METHODS

Bacterial strains, culture media and photofermentation set-up

The PNSB *Rhodobacter capsulatus* DSM155 (DSM155) and *R. capsulatus* B10 (B10) strains

were generously provided by the Laboratoire d'Electrochimie et Physicochimie des Matériaux et des Interfaces (LEPMI), Grenoble INP, Grenoble, France.

Reactivation, adaptation, growth, and hydrogen producing experiments were performed in RCV base medium (He et al. 2006), added with different compositions of acetic, butyric and lactic acids, along with different glutamate concentrations, according to experimental designs described below. Each liter of RCV base medium was prepared containing 50 mL of super salts medium (SSM), 20 mL of trace elements solution (TES), and buffer media (0.6 g/L KH_2PO_4 and 0.9 g/L K_2HPO_4). One liter of SSM medium consisted of 0.236 g $FeSO_4 \cdot 7H_2O$, 0.4 g EDTA ($C_{10}H_{14}N_2Na_2O_8 \cdot 2H_2O$), 1.5 g $CaCl_2 \cdot 2H_2O$, 4 g $MgSO_4 \cdot 7H_2O$, 0.02 g thiamine. TES medium was comprised by (1 L): 2.8 g de H_3BO_3, 1.592 g $MnSO_4 \cdot H_2O$, 0.04 g $CuSO_4 \cdot 5H_2O$, 0.24 g $ZnSO_4 \cdot 7H_2O$, and 0.752 g $Na_2MoO_4 \cdot 2H_2O$.

Addition of VFA to RCV base provided the media used for growth and hydrogen production evaluation. These were coined single-VFA, AB and ABL media. The composition of VFA were the following: single-VFA media contained either 30 mM acetic acid, 30 mM butyric acid, or 30 mM sodium lactate; the AB medium consisted of 16.6 mM acetic acid and 30 mM butyric acid; ABL medium was composed of 10 mM acetic acid, 20 mM butyric acid and 30 mM sodium lactate. The concentrations for the single-VFA experiments were chosen as these allow cell concentrations higher than 1 g/L in the adaptation cultures; additionally these are intermediate values amidst those used in literature for similar biological systems (Castillo-Moreno et al. 2018, Gadhamshetty et al. 2011), thus avoiding any risk of excess substrate inhibition or deficient hydrogen production due to low substrate concentration. The composition of AB medium respected the ratio 1.8 of butyric to acetic acid reported for the effluents of a dark fermentation process fed with sucrose (Rodríguez-Valderrama et al. 2019). The concentrations of VFA in ABL medium were chosen as an approximate to those found in the effluent of a 0.4 L UASB reactor fed with 31 g/L sucrose in semi-continuous operation. This reactor was inoculated with a granular sludge from a brewery wastewater treatment plant; the reactor was operated at room temperature, hydraulic retention time of 24 hours and organic load rate of 31 g/(L d). The pH of the media in all the cultures was adjusted to 6.9±0.1 with NaOH 5 M.

A photofermentation chamber was used for all the experiments as shown in **figure 1**. Light source was a high pressure sodium lamp (SILVANIA, USA), and light intensity (10, 20 or 30 klux) was set by
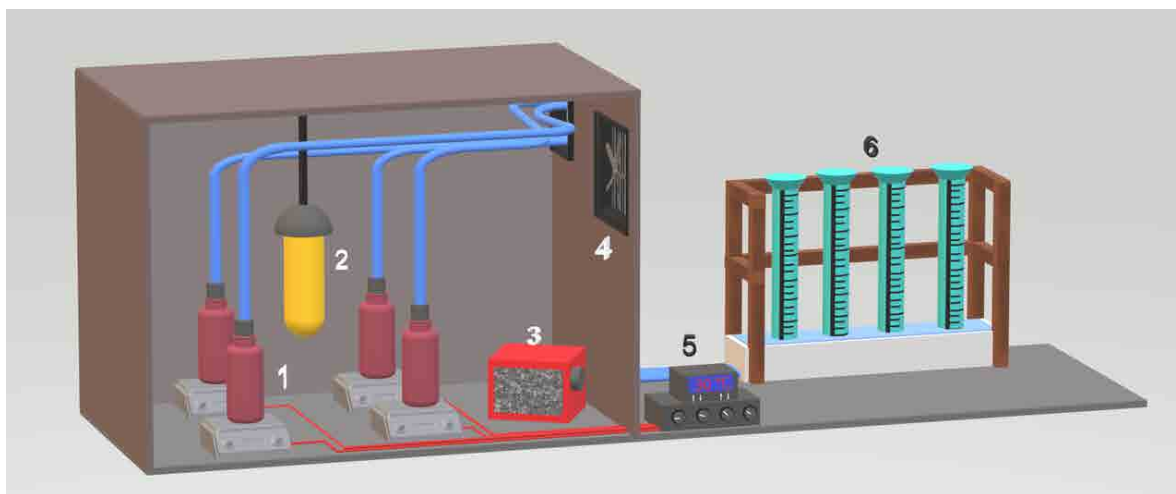
Fig. 1. Photofermentation chamber description. 1, flat-faced glass bottles and magnetic stirrer; 2, high sodium pressure lamp; 3, electric heater; 4, heat distributor; 5, stir and heat controller; 6, water displacement system.

spacing the bottles away from the lamp according to the measurement provided by a digital luxmeter (LX1010B, Alion).

Reactivation of both strains was performed in RCV base medium supplemented with 20 mM of sodium lactate and 7 mM of sodium glutamate, at 30 ºC and 30 klx of light intensity, in 15 mL sterile screwed glass test tubes.

Adaptation cultures were performed prior to hydrogen producing experiments. These cultures were grown in 15 mL sterile screwed glass test tubes at 30 °C and 30 klx using RCV base medium supplemented with single-VFA media (contained either 30 mM acetic acid, 30 mM butyric acid, or 30 mM sodium lactate) or ABL medium (composed of 10 mM acetic acid, 20 mM butyric acid and 30 mM sodium lactate).

Bacterial growth evaluation in organic acids media

DSM155 and B10 growth were evaluated using single-VFA and ABL media. All the assays were supplemented with sodium glutamate (10 mM) as nitrogen source. Experiments were run by duplicate in 15 mL sterile screwed glass test tubes at 30 °C and 30 klx.

Hydrogen production evaluation from volatile fatty acids media and light intensity variations

In this section, the hydrogen production was evaluated either varying VFA media, or the light intensity. First, AB and ABL media were evaluated for hydrogen production by DSM155 and B10 in sterile flat-faced glass bottles at 30 °C and 30 klx. Sodium glutamate concentration was 10 mM. Afterwards, the strain and medium showing the best hydrogen production were selected for the light intensity evaluation, performed at 10, 20, and 30 klx. Sodium glutamate concentration was 5 mM. The assays were started after inoculation of 3 mL of an adaptation culture (3 days of adaptation) to 107 mL of the corresponding medium in sterile conditions.

The flat-faced glass bottles (120 mL) were stirred individually by a magnetic stir bar. Experiments were run by duplicate.

Analytical methods

Bacterial growth was determined directly by the optical density at 660 nm in a spectrophotometer, whereas cell dry weight (CDW) was estimated according to the proportionality factor reported by (He et al. 2006) (absorbance equal to 1 is equivalent to 0.45 g dry weight). The biogas production was measured by water displacement method (**Fig. 1**), monitored using a computerized system equipped with cameras. The qualitative hydrogen determination was quantified using a permissible gas detector 8800 (TIF Instruments, INC).

Sodium lactate, acetic acid, and butyric acid concentrations after PF were quantified by high performance liquid chromatography (Agilent Technologies, 1260 Infinity, Refractive Index detector) using a Repromer H 9 μm column (250 x 8 mm, Ref RM9H0S2508) and a pre-column (Repromer H 9 μm, 20×8 mm, Ref RM9H0S0208), with H_2SO_4 (10 mM) as mobile phase.

The mobile phase flow rate and column temperatures were 1.0 mL/min and 60 °C, respectively. Before chromatographic analysis, the samples were first centrifugated (10000 g, 5 min), diluted 5-fold with distilled water, and filtered (Whatman nitrocellulose filter, 0.22 μm). Sodium lactate, butyric acid (Sigma-Aldrich), and acetic acid (J.T. Baker) were used as standards.

Kinetic models fitting

The experimental data of hydrogen production were fitted to different models to evaluate the hydrogen production performance parameters and analyze their differences and applications. The modified Gompertz model (Zwietering et al. 1990), the *Ti*-Gompertz model, and the sigmoidal Boltzmann model were used. The modified Gompertz model (Eq. 1) reads:

$$H(t) = H_{max} \cdot \exp\left\{-\exp\left[\frac{R_{max} \cdot e}{H_{max}}(\lambda - t) + 1\right]\right\}$$

where $H(t)$ (mL H_2) is cumulative hydrogen production as a time function, H_{max} (mL H_2) is the maximum cumulative hydrogen production, R_{max} (mL H_2/hour) is the maximum hydrogen production rate, λ (hours) is the lag time, t is any time (hours), and e is 2.718.

The *Ti*-Gompertz model (Eq. 2) reads:

$$H(t) = H_{max} \cdot \exp\left\{-\exp\left[\frac{R_{max} \cdot e}{H_{max}}(t - Ti)\right]\right\}$$

where Ti is the time at the inflection point (fixed at 36.79 % of the upper asymptote) (Tjørve and Tjørve, 2017).

Boltzmann's sigmoidal model was also used to determine the hydrogen production kinetic parameters (Eq. 3):

$$H(t) = H_{max} + \frac{\left(H_0 - H_{max}\right)}{\left(1 + \exp\left(\frac{(t - t_{50})}{dx}\right)\right)}$$

where H_0 is the initial hydrogen production (mL H_2), t_{50} is the time (hours) to reach half of H_{max} (mL H_2), and dx is the fit parameter related to the slope (hours).

For $H_0=0$ the R_{max} was determined using Eq. 4:

$$R_{max} = \frac{H_{max}}{4 \cdot dx}$$

The hydrogen molar pseudoyield (Y'_{H2} mol H_2/mol-$_{VFAconsumed}$) was determined in terms of total volatile fatty acids (TVFA) consumed according to Eq. 5 (Rodríguez-Valderrama et al. 2020b) to compare the photofermentation systems to the maximum theoretical hydrogen yields (6, 10, and 4 mol H_2/$_{mol organic acid}$ for lactate, butyrate, and acetate, respectively):

$$Y'_{H_2} = \frac{H_{max}}{V_R \cdot V_m \cdot \left(C_{VFA_0} - C_{VFA_f}\right) \cdot 1000}$$

where V_R is the fermentation volume (L), $C_{TVF,0}$ is the initial TVFA concentration (mol/L), $C_{VFA,f}$ is the final TVFA concentration (mol/L), V_M is the molar volume at standard reference conditions (22.4 L/mol H_2) and 1000 is the volume conversion factor (mL/L).

Two performance parameters to evaluate the efficiency of photofermentation amidst treatments are the substrate to hydrogen conversion efficiency, $\eta_{Substrate-H2}$ (%), and the light to hydrogen conversion efficiency, $\eta_{Light-H2}$ (%). The $\eta_{Substrate-H2}$ enables to assess how exhaustively was the substrate use in producing hydrogen. This parameter is determined as the ratio of the experimental hydrogen production (mL) over the theoretical production expected according to the stoichiometric conversion (Eq. 6):

$$\eta_{Substrate-H2} = \frac{H_{max}}{V_R \cdot V_M \cdot \left(Y_{Lac} \cdot C_{Lac,0} + Y_{But} \cdot C_{But,0} + Y_{Ace} \cdot C_{Ace,0}\right) \cdot 1000} \cdot 100$$

where Y_{lac} (6 mol H_2/mol$_{lactate}$), Y_{but} (10 mol H_2/mol$_{butyrate}$), Y_{ace} (4 mol H_2/mol$_{acetate}$) are the stoichiometric hydrogen yield for lactate, butyrate, and acetate, respectively. $C_{Lac,0}$, $C_{But,0}$ $C_{Ace,0}$ (mol/L) are the initial organic acid concentrations for lactate, butyrate, and acetate, respectively, and 1000 is the volume conversion factor (mL/L).

On the other hand, the light conversion efficiency, $\eta_{Light-H2}$ (%), contributes to the light performance evaluation since this parameter is a direct measure of the light use in the photofermentative hydrogen production (Basak et al. 2014). The $\eta_{Light-H2}$ is defined as the total energy in the form of hydrogen produced over the total energy input, as described in Eq. 7 (Miyake and Kawamura, 1987):

$$\eta_{Light-H2} = \frac{33.61 \cdot \rho_{H2} \cdot H_{max}}{I \cdot A \cdot t_f \cdot 1000} \cdot 100$$

where 33.61 is the hydrogen energy density (Wh/g), ρ_{H2} is hydrogen density (g/L), I is light intensity (W/m^2, 30 klx≈82 W/m^2, 20 klx≈51 W/m^2, 10 klx≈27 W/m^2), A is the irradiated area (m^2, 0.004 m^2), t_f is the final fermentation time (hours), and 1000 is the volume conversion factor (mL/L).

Statistics analysis

The Student's t-test was used to test the significant differences between the hydrogen production predicted parameters for *R. capsulatus* DSM155 and *R. capsulatus* B10 evaluated in the media ABL and AB (Montgomery 2012). One-way ANOVA with Tukey test was used to assess the significant differences between hydrogen production performance parameters at different light intensities, considering a confidence level of 95 %. The statistical analysis was evaluated using software package MINITAB 18 Statistical Sofware (Minitab Inc., State College, PA, USA).

RESULTS AND DISCUSSION

Bacterial growth evaluation in organic acids media

DSM155 and B10 were successfully grown using different carbon sources (**Table I**). The adaptation time for each growth medium was approximately 5 days. During the growth stage using single-VFA media, the highest cell growth for B10 (1.49 g/L) occurred when the medium contained acetic acid (30 mM), followed by butyric acid as shown in **Table I**; whereas for DSM155, the highest cell growth (1.29 g/L) was also presented for acetic acid medium. This behavior may be explained considering that the metabolic pathways of long-chain organic acids by PNSB are more complex than those of acetic acid, being acetic acid more easily assimilated than sodium lactate and butyric acid. Besides, the growth and hydrogen production from VFA by PNSB is carried out by the anaerobic cycle of light-dependent citric acid (TCA); in this cycle, the short-chain carbon sources can be easily converted to acetyl-CoA and enter directly into the TCA cycle (Shi and Yu, 2005).

On the other hand, ABL medium showed the highest CDW of 2.15 g/L for DSM155 and 1.67 g/L for B10 (**Table I**), despite the lower acetic acid concentration (10 mM) but higher overall VFA concentration (60 mM). The most noticeable improvement in CDW was that of DSM 155 that was ca. 40 % better than when acetic acid was used as a carbon source. This difference is mainly related to the increase in the carbon source availability, as shown by the higher C/N ratio in mix-VFA (16.3) compared to acetate medium (C/N=5.1); a higher C/N ratio leads to preferred biomass production over hydrogen production (Ghosh et al. 201, Oliveira et al. 2014).

The considerable effect of the growth of initial carbon concentration and organic acids composition on PNSB growth has been demonstrated in the literature. Uyar et al. (2009) found differences of 33.3 % (CDW=1.6 g/L; 30 mM acetate) and 50 % (CDW=1.2 g/L; 20 mM lactate) in the growth of *R. sphaeroïdes* O.U. 001 (DSM 5864) when they analyzed the initial concentration and type of organic acid and compared it with a mixture of organic acids (CDW=2.4 g/L; 40 mM acetate, 10 mM butyrate, and 5 mM propionate) for hydrogen production in photobioreactors (55 mL) at 30-33 °C irradiated with a 100 W tungsten lamp (150-200 W/m^2) using sodium glutamate (10 mM) as nitrogen source.

Evaluation of hydrogen production from volatile fatty acids media and light intensity effect

DSM155 showed the best use of mix-VFA for hydrogen production. Indeed, the highest H_{max} for DSM155 and B10 were obtained using ABL medium, 239.2 mL H$_2$ and 209.6 mL H$_2$, respectively (**Table II, Fig. 2**). This result was statistically significant (*t-Student* confidence level of 95 %, $p<0.05$, **Table SI**). The ABL medium favored 35 to 37 % higher H_{max} than the AB medium, which may be ascribed to the 22.3 % additional carbon source in the ABL medium, represented by lactate, which also

TABLE I. DSM155 AND B10 GROWTH IN SINGLE-VFA AND ABL MEDIA.

Medium	VFA initial concentration	DSM155	B10
		CDW (g/L)	CDW (g/L)
Single-VFA	Sodium lactate (30 mM)	0.90±0.13	0.68±0.06
	Acetic acid (30 mM)	1.29±0.07	1.49±0.05
	Butyric acid (30 mM)	0.90±0.19	0.86±0.12
ABL	Sodium lactate (30 mM) Butyric acid (20 mM) Acetic acid (10 mM)	2.15±0.23	1.67±0.17

promotes hydrogen production in photofermentative processes even in no light conditions (Ghosh et al. 2017, Lazaro et al., 2017).

Our results are in good agreement to literature as differences in H_{max} are expected in function of the carbon source concentration and composition (single acid or acid mixtures) and photofermentative strains. Akman et al. (2015) demonstrated that *R. capsulatus* DSM 1710 increased hydrogen production from 80 mL H_2 to 143 mL H_2 (55.9 %)
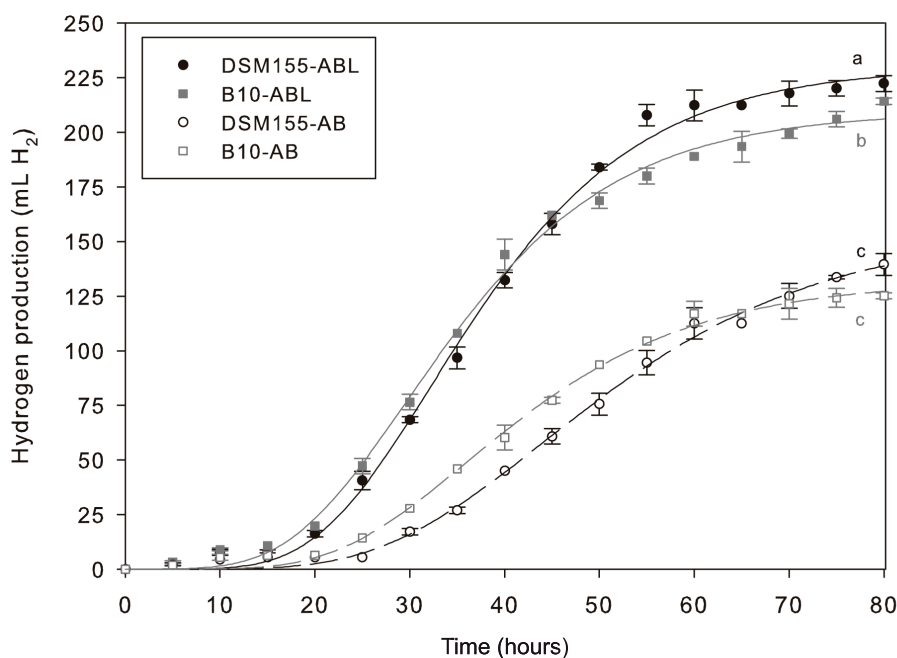
Fig. 2. Cumulative hydrogen production by DSM155 and B10 on ABL and AB media at 10 mM of sodium glutamate. Solid and long dash lines correspond to the fit to modified Gompertz model. Values statistically significant from others are shown with different letters.

TABLE II. MODIFIED GOMPERTZ MODEL AND PERFORMANCE PARAMETERS OF HYDROGEN PRODUCTION FROM MEDIUM ABL AND AB.

Parameter	DSM155		B10	
	ABL medium	AB medium	ABL medium	AB medium
$H_{max\text{-}exp}$ (mL H_2)	222.30	139.50	214.20	125.10
H_{max} (mL H_2)	**239.20**	156.32	**209.60**	132.33
R_{max} (mL H_2/hours)	6.92	3.40	6.26	3.58
λ (hours)	20.14	27.01	17.40	22.32
R^2	0.998	0.997	0.997	0.997
Adjusted R^2	0.997	0.996	0.996	0.997
Error (%)	7.60	12.06	2.14	5.78
CDW (g/L)	2.39	1.99	0.90	0.65
V_p	2174.5	1421.1	1905.5	1203.0
Y'_{H_2} (mol H_2/molVFA consumed)	2.27	2.14	2.25	1.95
Organic acid consumption (%)	L:65.7 A:51.9 B:89.5	B:56.7 A:75.9	L:56.7 A:47.9 B:79.8	B:53.3 A:69
$\eta_{Substrate\text{-}H2}$ (%)	23.11	17.31	20.25	14.66

Notes: A, acetate; B, butyrate; L, lactate, V_p, volumetric productivity. The significant difference ($p<0.05$) determined by *t*-student for H_{max} and R_{max} was evaluated for each media and strain, values statistically significant from others are shown in bold letters.

by increasing acetate concentration by 66 % (20 to 60 mM), in 55 mL glass bottles photobioreactors at 30 °C and 200 W/m^2 (3000 lx). On the other hand, for binary mixtures of organic acids, Chen et al. (2008) reported a 42.6 % increase in H_{max} (1506 mL H$_2$ to 2625 mL H$_2$) when the initial concentration of organic acids increased from 18.4 mM (1.2 butyric/acetate ratio) to 62.8 mM (1.2 butyric/acetate ratio) with *Rhodopseudomonas palustris* WP3-5 in 1 L photobioreactor at 95 W/m^2 and 32 °C. Besides, Shi and Yu (2006) reported a higher H_{max} of 267.0 mL H$_2$ using mix-VFA medium (31. 6 mM, acetate; 5.4 mM, propionate; 9.1 mM, butyrate) than the 208.3 mL H$_2$ produced with acetate (27.3 mM), and 197.0 mL H$_2$ with butyrate (25 mM) by *Rhodopseudomonas capsulata* in 300 mL glass vials at 32 °C and 4 klx. According to the above demonstrated, it is inferred that photofermentation can be coupled to dark fermentation hydrogen production, allowing the effective use of VFA-rich effluents and thus increasing the overall hydrogen production.

The R_{max} for DSM155 and B10 showed no significant difference (6.9 ± 0.3 and 6.2 ± 0.3 mL H$_2$/hour, respectively, p=0.244, **Table SI**). The evaluation of H_{max} and R_{max} is important since H_{max} gives an idea of the maximum accumulation of hydrogen of the system (performance indicator), and R_{max} is a critical parameter for bioreactors design in fermentative hydrogen production (Chen et al. 2008).

The H_{max} and R_{max} are comparable with Gompertz parameters for different strains of PNSB at 10 mM of nitrogen source. Hu et al. (2018) reported H_{max} and R_{max} for single VFA (lactate; H_{max}, 50.12 mL H$_2$ and R_{max}, 0.25 mL H$_2$/hour and butyrate; $_{Hmax}$, 40.7 mL H$_2$ and R_{max}, 0.43 mL H$_2$/hour) using 10 mM sodium glutamate with *R. palustris* in 0.03 L serum bottles at 30 °C and 2 klx (incandescent bulbs). The values presented by Hu et al. (2018) were relatively lower than those presented in this study, mainly due to the low light intensity applied, long adaptation times (λ=40 hours for lactate and λ=722.3 hours for butyrate) compared to malate (λ=16.2 hours), and under these conditions biomass production dominated over hydrogen production (OD=3.52 for lactate and OD=1.57 for butyrate).

The molar pseudoyields were in the range 2.25-2.27 mol H$_2$/mol$_{VFAconsumed}$ for DSM155 and 1.95-2.24 for B10. Regarding the R_{max}, no significant differences were found for Y'_{H2} between photofermentative strains evaluated for ABL media (p=0.771, **Table SI**) and AB (p=0.137, **Table SII**). This demonstrates the ability of the two photofermentative strains to transform mixed sources of organic acids into hydrogen. Similar yields were found in the literature. Ren et al. (2008) reported a molar yield (Y_{H2}) in terms of total

volatile fatty acids added of 1.71 mol H$_2$/mol$_{TVFA-}$ added when they evaluated hydrogen production with *Rhodopseudomonas faecalis* RLD-53 at initial concentration of 25 mM acetate and 25 mM butyrate in 0.08L reactors at 35 °C, 4 klx, and 10 mM of sodium glutamate. Moreover, Cardeña et al. (2015) reported a Y_{H2} of 2.26 mol H$_2$/mol$_{TVFAadded}$ using a photofermentative consortium at 30-35 °C and 5 klx at initial concentration of organic acid mixture of 20 mM acetate, 10 mM propionate, and 18 mM butyrate.

In addition, although the organic acids consumption for ABL and AB media is between 63.9-71.3 % and 59.2-63.5 %, respectively, the η$_{Substrate-H2}$ values were relatively low (14.66-17.31 % for AB medium, and 20.25-23.11 % for ABL medium, **Table II)** compared to those reported in the literature for hydrogen production with single ($\eta_{Substrate-H2}$=69 %, 35 mM acetate) (Tao et al. 2008), binary ($\eta_{Substrate-H2}$=85.6 %, 25 mM acetate, and 25 mM butyrate) (Ren et al. 2008) and ternary media ($\eta_{Substrate-H2}$=34 %, 31. 6 mM acetate, 5.4 mM propionate, and 9.1 mM butyrate) (Shi and Yu 2006). The reasons could be ascribed to the deviation of the carbon source for cell growth and maintenance, likely influenced by the high glutamate concentration (10 mM) since the nitrogen source concentration strongly influences the hydrogen production efficiency. In that sense, decreasing the nitrogen source concentration will increase the H_{max}, Y'_{H2}, and $\eta_{Substrate-H2}$.

Effect of light intensity on hydrogen production

The effect of light intensity on hydrogen production was evaluated using DSM155 strain according to the results of the previous section. Besides, as an enhancement strategy for hydrogen production, the sodium glutamate concentration in this series of experiments was reduced from 10 to 5 mM.

The cumulative hydrogen production and its different fitting models (solid lines) as a function of time for the different light intensities using DSM155 are shown in **figure 3**. According to the H_{max} and R_{max} predicted by the two models, as the light intensity increased (from 10 to 30 klx), the H_{max} and R_{max} also increased (**Fig. 3, Table III**); which is mainly due to the light availability as an ambivalent factor for increasing or limiting biohydrogen formation. At low light intensities the minimum threshold to start the bacterial growth would be insufficient (Lazaro et al. 2015). For *R. capsulatus* B10, the effect of light intensity has been evaluated by Castillo et al. (2012), who found that as light intensity increases from 8 to 23.6 klx, the hydrogen production increases from 264 mL H$_2$ to 654 mL H$_2$ with lactate (120 mM) as
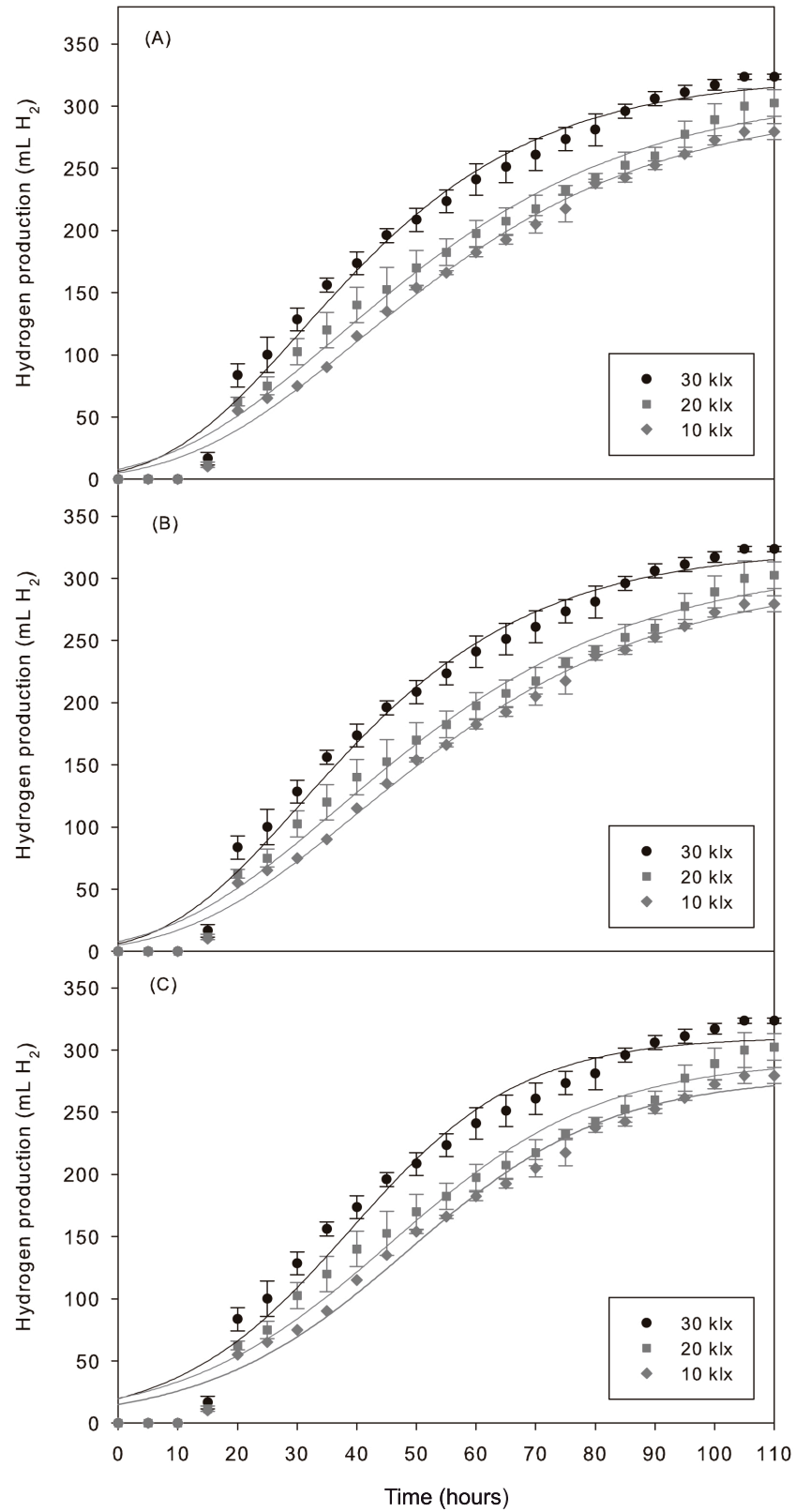
Fig. 3. Cumulative hydrogen production from ABL at different light intensities by DSM155 for (A) Gompertz model, (B) Gompertz-Ti model, (C) Boltzmann (H_0=0) model.

carbon source at 30 °C; additionally, they reported that from 23.6 klx onwards the saturation light intensity values are presented, so that hydrogen productions decreased down to 524 mL H_2 at 30 klx light intensity. On the other hand, the inhibitory light intensities may vary between strains of the same species, as it depends mainly on the photo-adaptation capacity of each microorganism (Gadhamshetty et al. 2011).

According to the kinetic model parameters estimated after 110 hours of fermentation (**Table III**), the H_{max} for the three models was in the range 310.49-324.09 mL H_2 for the experiment carried out at 30 klx, whereas for those developed at 20 and 10 klx, the H_{max} was between 292.01 to 313.55 mL H_2, and 278.50 to 302.88 mL H_2, respectively. The maximum predicted H_{max} (324.09 mL H_2) was

TABLE III. KINETIC PARAMETERS OF FITTING MODELS ON THE MAXIMUN CUMULATIVE HYDROGEN PRODUCTION OF ORGANIC ACID MIXTURE BY DSM155 AT DIFFERENT LIGHT INTENSITIES.

Model	Light intensity	Model parameters	Experimental H_{max} and error	Vp mL H_2/L_{op}	Y'_{H2} (mol H_2/mol-VFAconsumed)	$\eta_{Substrate-H2}$ (%)	$\eta_{Light-H2}$ (%)
	30 klx	H_{max}=324.09 R_{max}= **5.36** λ= 8.35	$H_{max-exp}$= 323.5 Error (%)= 0.18	2946.3	3.10	3.10	**2.67**
Gompertz	20 klx	H_{max} = 313.55 R_{max} = 4.07 λ= 8.62	$H_{max-exp}$= 302.5 Error (%)= 3.65	2850.5	2.64	2.64	**4.16**
	10 klx	H_{max} = 302.88 R_{max} = 3.90 λ= 11.68	$H_{max-exp}$= 279.5 Error (%)= 8.36	2753.5	3.17	3.17	**7.47**
	30 klx	H_{max} = 324.09 R_{max} = **5.36** Ti= 30.71	$H_{max-exp}$= 323.5 Error (%)= 0.18	2946.3	3.10	31.32	**2.67**
Gompertz-Ti	20 klx	H_{max} = 313.55 R_{max} = 4.07 Ti= 36.96	$H_{max-exp}$= 302.5 Error (%)= 3.65	2850.5	2.64	30.30	**4.16**
	10 klx	H_{max} = 302.88 R_{max} = 3.90 Ti= 40.25	$H_{max-exp}$= 279.5 Error (%)= 8.36	2753.5	3.17	29.28	**7.47**
	30 klx	H_{max} = 310.49 dx= 14.44 t_{50}= 38.89 R_{max} = 5.42	$H_{max-exp}$= 323.5 Error (%)= 4.02	2822.6	3.03	**30.63**	2.55
Boltzmann H_0=0	20 klx	H_{max} = 292.01 dx= 17.50 t_{50}= 45.94 R_{max} = 4.63	$H_{max-exp}$= 302.5 Error (%)= 3.47	2654.6	**2.51**	28.72*	**3.88**
	10 klx	H_{max}= 278.50 d_x= 16.94 t_{50}= 48.72 R_{max} = 4.13	$H_{max-exp}$= 279.5 Error (%)= 0.36	2531.8	2.92	**26.96**	6.87

Notes: R^2 and adjusted R^2 values are ranged between 0.9734-0.9952 and 0.9691-0.9942, respectively. $H_{max-exp}$, maximum experimental cumulative hydrogen production (mL H_2); H_{max}, (mL H_2); R_{max}, (mL H2/h); λ, (h); Ti, (h); dx, (h); t_{50}, (h); h_0, (mL H_2); V_p, volumetric productivity. The significant difference ($p<0.05$) was evaluated for each column and model. Values statistically significant from others are shown in bold letters; * in the Boltzman model at 20 klx shows a value that was not significantly different from the value from above or below.

found for the Gompertz model at 30 klx, and this fit presented the lowest deviation (0.18 %) from the experimental value, compared to the H_{max} values predicted by the Boltzmann model (4.02 %) at 30 klx (**Table III**). According to the analysis of variance, the H_{max} from the different light intensity assays for either the modified Gompertz (**Table SIII**), Gompertz-*Ti* (**Table SIII**), and Boltzmann (**Table SV**) models did not show significant differences, so that the H_{max} is not statistically influenced by the light intensity variation. The results show that DSM155 had an excellent performance in hydrogen production from mix-VFA medium in the light intensities range from 10 to 30 klx; this enables to extend the working light intensities range and operate the photofermentative system in limited light conditions without compromising the bioprocess performance.

Similar to H_{max}, the predicted values of R_{max} with the Gompertz (3.90-5.36 mL H_2/hour) and Boltzmann (4.13-5.42 mL H_2/hour) models increased as light intensity did (10-30 klx) (**Table III**), respectively. The variance analysis for predicted R_{max} shows significant differences with the modified Gompertz and Gompertz-*Ti* model at different light intensities, while for the Boltzmann model, no significant differences were found. According to the Tukey test, the predicted R_{max} for 30 klx presented a slight difference in respect to the values for 10 and 20 klx. This shows that light intensity acts as a crucial factor for R_{max} variation.

The Y'_{H2} calculated with Eq. 5 were between 2.51-3.17 mol H_2/mol$_{VFAconsumed}$. The highest Y'_{H2} was found for the experiment at 10 klx (3.17 mol H_2/mol$_{VFAconsumed)}$ for Gompertz and Gompertz-*Ti* models; however, the ANOVA for the Y'_{H2} did not show significant differences. On the contrary, the Y'_{H2} obtained by the Boltzmann model showed significant differences, being 3.03 and 2.92 mol H_2/mol$_{VFAconsumed}$ (from 30 and 10 klx, respectively), significantly different with respect to 2.51 mol H_2/mol$_{VFAconsumed}$ from 20 klx. These values are comparable with yields reported in the literature for photofermentation systems. Sevinç et al. (2012) found a Y_{H2} of 1.32 mol H_2/mol$_{TVFAadded}$ when they evaluated the hydrogen production (3 klx, 30 °C) by *Rhodobacter capsulatus* DSM 1710 from acetic acid (40 mM) and lactic acid (7.5 mM) mixture. Conversely, in the case of Obeid et al. (2009) who reported a Y'_{H2} of 2.9 mol H_2/mol$_{TVFAadded}$ when they analyzed the hydrogen production (30 klx, 30 °C) using sodium lactate (80 mM) by *Rhodobacter capsulatus* IR3. On the other hand, with

R. capsulatus DSM 155, a yield of 0.6 mol H_2/mol$_{acetate}$ was reported by Gebicki et al. (2010) when evaluated the hydrogen production in a panel reactor (100 L) sunlight irradiated using acetic acid as carbon source (23 mM).

The substrate to hydrogen conversion efficiency ($\eta_{Substrate-H2}$) by DSM155 was also influenced by illumination intensity, as it increased when light intensity raised from 10 to 30 klx (**Table III**). The ANOVA for $\eta_{Substrate-H2}$ determined with the Gompertz adjustment showed no significant differences, whereas those determined with the Boltzmann model showed significant differences. According to the statistical comparison with Tukey test, the $\eta_{Substrate-H2}$ (30.63 %) at 30 klx is significantly different from the $\eta_{Substrate-H2}$ (26.93 %) at 10 klx; however, the $\eta_{Substrate-H2}$ (28.72 %) at 20 klx is not significantly different from the $\eta_{Substrate-H2}$ at 30 and 10 klx. This difference between $\eta_{Substrate-H2}$ at 30 and 10 klx is related to the ATP and reductive power availability present in the photosynthetic system at high intensities and below the saturation intensity, which is necessary to favor the hydrogen production (Gadhamshetty et al. 2011). Comparing the $\eta_{Substrate-H2}$ in equality of conditions with those reported in the literature is intricate because this parameter depends strongly on photosynthetic strains, carbon sources (mixed or simple), and experimental conditions (Trchounian 2015). However, the effect of light intensity on $\eta_{Substrate-H2}$ has been demonstrated in the study realized by Tao et al. (2008) where they found that $\eta_{Substrate-H2}$ increased from 26.89 % to 71.25 % when they varied light intensity from 1.5 klx to 5 klx in hydrogen production from malate (30 mM) with *R. sphaeroides* ZX-5 at 30 °C.

The effect of light intensity on $\eta_{Light-H2}$ was inversely proportional, as shown in **Table III**. The $\eta_{Light-H2}$ reached maximum values (7.47 %, Gompertz model; 6.87 %, Boltzmann model) at the lowest light intensity evaluated (10 klx), meanwhile, when the intensity increased up to 30 klx, the $\eta_{Light-H2}$ reached minimum values (2.67 %, Gompertz model; 2.55 %, Boltzmann model). According to the ANOVA for $\eta_{Light-H2}$ comparing Gompertz and Boltzmann models, there were no significant differences between the $\eta_{Light-H2}$ at 30 klx, 20 klx, and 10 klx, despite the higher values predicted by Gompertz.

At different light intensities, the Gompertz and Boltzmann model comparison showed significant differences, thus inferring that the intensity plays an important role in the $\eta_{Light-H2}$ because $\eta_{Light-H2}$ is low when the energy capacity supplied to the

hydrogen-producing enzyme (nitrogenase) is exceeded (Carlozzi 2009).

CONCLUSION

R. capsulatus DSM155 and *R. capsulatus* B10 were efficiently adapted to acetic acid, butyric acid, and sodium lactate containing media, obtaining the highest CDW when grown on ABL medium. Moreover, both strains were able to produce hydrogen from AB and ABL media, being higher with the latter. *R. capsulatus* DSM155 was able to produce hydrogen in a range of light intensities between 10 to 30 klx. Overall, *R. capsulatus* DSM155 presented the highest performance on hydrogen production at 30 klx using ABL medium in terms of the H_{max}, R_{max}, and $\eta_{Substrate-H2}$ were 324.09 mL H_2, 5.36 mL H_2/hour, and 31.32 %, respectively. It is noteworthy that 10 klx light intensity presented the highest Y'_{H2} and $\eta_{Light-H2}$ (3.17 mol H_2/mol$_{VFAconsumed}$ and 7.47 %, respectively) despite presenting less than 7 % lower H_{max} and $\eta_{Substrate-H2}$ compared to those at 30 klx. Gompertz and Boltzmann models adjusted adequately to the biohydrogen photofermentation performance; minor and expectedly statistical differences in H_{max}, R_{max}, Y'_{H2}, and $\eta_{Substrate-H2}$ were found amidst them when comparing the different light intensities.

This study demonstrated the ability of DSM155 and B10 strains of *Rhodobacter capsulatus* to produce hydrogen from organic acid mixtures, which is a step forward in application of organic acid-rich real effluents for photofermentative hydrogen production systems.

ACKNOWLEDGMENTS

ABBREVIATIONS

A	irradiated area (m^2)
AD	anaerobic digestion
CDW	cell dry weight (g/L)

$C_{Ace,0}$	initial organic acid concentrations for acetate (mol/L)
$C_{But,0}$	initial organic acid concentrations for butyrate (mol/L)
$C_{Lac,0}$	initial organic acid concentrations for lactate (mol/L)
$C_{TVF,0}$	initial TVFA concentration (mol/L)
$C_{VFA,f}$	final TVFA concentration (mol/L)
DF	dark fermentation
dx	fit parameter related to the slope (h)
e	Euler number (2.718)
H_0	initial hydrogen production (mL H_2)
$H(t)$	cumulative hydrogen production at time 't' (mL H_2)
H_{max}	maximum cumulative hydrogen production (mL H_2)
I	light intensity (W/m^2)
PF	photofermentation
PNSB	purple non-sulfur bacteria
R_{max}	maximum hydrogen production rate (mL H_2/hour)
SSM	super salts medium
TES	trace elements solution
t_{50}	time (hours) to reach half of H_{max} (mL H_2)
t	time (hours)
t_f	final fermentation time (hours)
Ti	time at the inflection point (hours)
TVFA	total volatile fatty acids
UASB	upflow anaerobic sludge blanket
VFA	volatile fatty acids
V_M	molar volume at standard reference conditions (22.4 L/mol H_2)
V_R	fermentation volume (L)
Y_{ace}	stoichiometric hydrogen yield for acetate (4 mol H_2/mol$_{acetate}$)
Y_{but}	stoichiometric hydrogen yield for butyrate (10 mol H_2/mol$_{butyrate}$)
Y_{H2}	hydrogen molar yield (mol H_2/mol$_{TVFAadded}$)
Y'_{H2}	hydrogen molar pseudoyield (mol H_2/mol$_{VFAconsumed}$)
Y_{lac}	stoichiometric hydrogen yield for lactate (6 mol H_2/mol$_{lactate}$)
λ	
V_p	Volumetric productivity (mL H_2/L$_{op}$)

Greek characters

λ	lag time (hours)
ρ_{H2}	hydrogen density (g/L)
$\eta_{Substrate-H2}$	substrate to hydrogen conversion efficiency (%)
$\eta_{Light-H2}$	light to hydrogen conversion efficiency (%)

REFERENCES

Akman M. C., Erguder, T. H., Gündüz, U., and Eroglu, I. (2015). Investigation of the effects of initial substrate and biomass concentrations and light intensity on photofermentative hydrogen gas production by response surface methodology. Int. J. Hydrogen Energy 40 (15), 5042–5049. https://doi.org/10.1016/j.ijhydene.2015.02.093

Argun H., and Kargi, F. (2011). Bio-hydrogen production by different operational modes of dark and photo-fermentation: An overview. Int. J. Hydrogen Energy 36 (13), 7443–7459. https://doi.org/10.1016/j.ijhydene.2011.03.116

Basak N., Jana, A. K., Das, D., and Saikia, D. (2014). Photofermentative molecular biohydrogen production by purple-non-sulfur (PNS) bacteria in various modes: The present progress and future perspective. Int J Hydrogen Energy 39 (13), 6853–6871. https://doi.org/10.1016/j.ijhydene.2014.02.093

Cardeña R., Moreno, G., Valdez-Vazquez, I., and Buitrón, G. (2015). Optimization of volatile fatty acids concentration for photofermentative hydrogen production by a consortium. Int. J. Hydrogen Energy 40 (48), 17212–17223. https://doi.org/10.1016/j.ijhydene.2015.10.020

Carlozzi P. (2009). The effect of irradiance growing on hydrogen photoevolution and on the kinetic growth in Rhodopseudomonas palustris, strain 42OL. Int. J. Hydrogen Energy 34 (19), 7949–7958. https://doi.org/10.1016/j.ijhydene.2009.07.083

Castillo P., Magnin, J. P., Velasquez, M., and Willison, J. (2012). Modeling and optimization of hydrogen production by the photosynthetic bacterium rhodobacter capsulatus by the methodology of Design of Experiments (DOE): Interaction between lactate concentration and light luminosity. Energy Procedia 29, 357–366. https://doi.org/10.1016/j.egypro.2012.09.042

Chen C. Y., Lu, W. Bin, Liu, C. H., and Chang, J. S. (2008). Improved phototrophic H2 production with Rhodopseudomonas palustris WP3-5 using acetate and butyrate as dual carbon substrates. Bioresour. Technol. 99 (9), 3609–3616. https://doi.org/10.1016/j.biortech.2007.07.037

Gadhamshetty V., Sukumaran, A., and Nirmalakhandan, N. (2011). Review: Photoparameters in photofermentative biohydrogen production. Crit. Rev. Environ. Sci. Technol. 41 (1), 1–51. https://doi.org/10.1080/10643380802502011

Gebicki J., Modigell, M., Schumacher, M., Van Der Burg, J., and Roebroeck, E. (2010). Comparison of two reactor concepts for anoxygenic H2 production by Rhodobacter capsulatus. J. Clean Prod. 18 (Suppl. 1), S36–S42. https://doi.org/10.1016/j.jclepro.2010.05.023

Ghosh, S., Dairkee, U. K., Chowdhury, R., and Bhattacharya, P. (2017). Hydrogen from food processing wastes via photofermentation using Purple Non-sulfur Bacteria (PNSB) – A

review. Energy Conv. Manag. 141, 299–314. https://doi.org/10.1016/0360-3199(87)90146-7

He D., Bultel, Y., Magnin, J., and Willison, J. C. (2006). Kinetic analysis of photosynthetic growth and photohydrogen production of two strains of Rhodobacter Capsulatus. Enzyme Microb. Technol. 38 (1-2), 253–259. https://doi.org/10.1016/j.enzmictec.2005.06.012

Hu C., Choy, S. Y., and Giannis, A. (2018). Evaluation of Lighting Systems, Carbon Sources, and Bacteria Cultures on Photofermentative Hydrogen Production. Appl. Biochem. Biotechnol. 185 (1), 257–269. https://doi.org/10.1007/s12010-017-2655-5

Keskin T., Abo-Hashesh, M., and Hallenbeck, P. C. (2011). Photofermentative hydrogen production from wastes. Bioresour. Technol. 102 (18), 8557–8568. https://doi.org/10.1016/j.biortech.2011.04.004

Lazaro C. Z., Hitit, Z. Y., and Hallenbeck, P. C. (2017). Optimization of the yield of dark microaerobic production of hydrogen from lactate by Rhodopseudomonas palustris. Bioresour. Technol. 245, 123–131. https://doi.org/10.1016/j.biortech.2017.08.207

Lazaro C. Z., Varesche, M. B. A., and Silva, E. L. (2015). Effect of inoculum concentration, pH, light intensity and lighting regime on hydrogen production by phototrophic microbial consortium. Renew. Energy 75, 1–7. https://doi.org/10.1016/j.renene.2014.09.034

Magnin J. P., and Deseure, J. (2019). Hydrogen generation in a pressurized photobioreactor: Unexpected enhancement of biohydrogen production by the phototrophic bacterium Rhodobacter capsulatus. Appl. Energy 239 , 635–643. https://doi.org/10.1016/j.apenergy.2019.01.204

Miyake J., and Kawamura, S. (1987). Efficiency of light energy conversion to hydrogen by the photosynthetic bacterium Rhodobacter sphaeroides. Int. J. Hydrogen Energy 12 (3), 147–149. https://doi.org/10.1016/0360-3199(87)90146-7

Montgomery D. C. (2012). Design and Analysis of Experiments. 8th Ed, Wiley, New Jersey.

Mu Y., Yu, H. Q., and Wang, G. (2007). A kinetic approach to anaerobic hydrogen-producing process. Water Res. 41 (5), 1152–1160. https://doi.org/10.1016/j.watres.2006.11.047

Obeid J., Magnin, J. P., Flaus, J. M., Adrot, O., Willison, J. C., and Zlatev, R. (2009). Modelling of hydrogen production in batch cultures of the photosynthetic bacterium Rhodobacter capsulatus. Int. J. Hydrogen Energy 34 (1), 180–185. https://doi.org/10.1016/j.ijhydene.2008.09.081

Oliveira T. V, Bessa, L. O., Oliveira, F. S., Ferreira, J. S., Batista, F. R. X., and Cardoso, V. L. (2014). Insights into the effect of carbon and nitrogen source on hydrogen production by photosynthetic bacteria. Chem. Eng. Trans. 38, 367–372. https://doi.org/10.3303/CET1438062

Ren N. Q., Liu, B. F., Ding, J., Guo, W. Q., Cao, G. L., and Xie, G. J. (2008). The effect of butyrate concentration

on photo-hydrogen production from acetate by Rhodopseudomonas faecalis RLD-53. Int. J. Hydrogen Energy, 33 (21), 5981–5985. https://doi.org/10.1016/j.ijhydene.2008.07.020

Rodríguez-Valderrama S., Escamilla-Alvarado, C., Amezquita-Garcia, H. J., Cano-Gómez, J. J., Magnin, J. P., and Rivas-García, P. (2019). Evaluation of feeding strategies in upflow anaerobic sludge bed reactor for hydrogenogenesis at psychrophilic temperature. Int. J. Hydrogen Energy 44 (24), 12346–12355. https://doi.org/10.1016/j.ijhydene.2018.09.215

Rodríguez-Valderrama S., Escamilla-Alvarado, C., Magnin, J. P., Rivas-García, P., Valdez-Vazquez, I., and Ríos-Leal, E. (2020a). Batch biohydrogen production from dilute acid hydrolyzates of fruits-and-vegetables wastes and corn stover as co-substrates. Biomass Bioenergy 140, 105666. https://doi.org/10.1016/j.biombioe.2020.105666

Rodríguez-Valderrama S., Escamilla-Alvarado, C., Rivas-García, P., Magnin, J., Alcalá-Rodríguez, M., and García-Reyes, R. B. (2020b). Biorefinery concept comprising acid hydrolysis, dark fermentation , and anaerobic digestion for co-processing of fruit and vegetable wastes and corn stover. Environ. Sci. Pollut. Res. 27, 28585–28596. https://doi.org/10.1007/s11356-020-08580-z

Sevinç P., Gündüz, U., Eroglu, I., and Yücel, M. (2012). Kinetic analysis of photosynthetic growth, hydrogen production and dual substrate utilization by Rhodobacter capsulatus. Int. J. Hydrogen Energy 37 (21), 16430–16436. https://doi.org/10.1016/j.ijhydene.2012.02.176

Shi X. Y., and Yu, H. Q. (2006). Conversion of individual and mixed volatile fatty acids to hydrogen by Rhodopseudomonas capsulata. Int. Biodeterior. Biodegrad. 58 (2), 82–88. https://doi.org/10.1016/j.ibiod.2006.07.004

Shi X. Y., and Yu, H. Q. (2005). Response surface analysis on the effect of cell concentration and light intensity on hydrogen production by Rhodopseudomonas capsulata. Process Biochem. 40 (7), 2475–2481. https://doi.org/10.1016/j.procbio.2004.09.010

Tao Y., He, Y., Wu, Y., Liu, F., Li, X., Zong, W., and Zhou, Z. (2008). Characteristics of a new photosynthetic bacterial strain for hydrogen production and its application in wastewater treatment. Int. J. Hydrogen Energy 33 (3), 963–973. https://doi.org/10.1016/j.ijhydene.2007.11.021

Tiang M. F., Fitri Hanipa, M. A., Abdul, P. M., Jahim, J. M. d., Mahmod, S. S., Takriff, M. S., Lay, C. H., Reungsang, A., and Wu, S. Y. (2020). Recent advanced biotechnological strategies to enhance photo-fermentative biohydrogen production by purple non-sulphur bacteria: An overview. Int. J. Hydrogen Energ, 45 (24), 13211–13230. https://doi.org/10.1016/j.ijhydene.2020.03.033

Tjørve K. M. C., and Tjørve, E. (2017). The use of Gompertz models in growth analyses, and new Gompertz-model approach: An addition to the Unified-Richards family. PLoS One 12 (6), 1–17. https://doi.org/10.1371/journal.pone.0178691

Trchounian A. (2015). Mechanisms for hydrogen production by different bacteria during mixed-acid and photo-fermentation and perspectives of hydrogen production biotechnology. Crit. Rev. Biotechnol. 35 (1), 103–113. https://doi.org/10.3109/07388551.2013.809047

Uyar B., Eroglu, I., Yücel, M., and Gündüz, U. (2009). Photofermentative hydrogen production from volatile fatty acids present in dark fermentation effluents. Int. J. Hydrogen Energy 34 (10), 4517–4523. https://doi.org/10.1016/j.ijhydene.2008.07.057

Wang J., and Wan, W. (2009). Kinetic models for fermentative hydrogen production: A review. Int J Hydrogen Energy 34 (8), 3313–3323. https://doi.org/10.1016/j.ijhydene.2009.02.031

Zwietering M. H., Jongenburger, I., Rombouts, F. M., and Van 't Riet, K. (1990). Modeling of the bacterial growth curve. Appl. Environ. Microbiol. 56 (6), 1875–1881. https://doi.org/10.1128/aem.56.6.1875-1881.1990

SUPPLEMENTARY INFORMATION

TABLE SI. T-STUDENT COMPARISON FOR THE PREDICTED PARAMETERS IN THE HYDROGEN PRODUCTION BY *R. CAPSULATUS* DSM 155 (DSM155) AND *R. CAPSULATUS* B10 (B10) EVALUATED IN THE MEDIA ABL.

Parameter	*t-value*	DF	*p-value*
H_{max}	6.25	2	0.025
R_{max}	1.63	2	0.244
Y'_{H2}	0.33	2	0.771

TABLE SII. T-STUDENT COMPARISON FOR THE PREDICTED PARAMETERS IN THE HYDROGEN PRODUCTION BY DSM155 AND B10 EVALUATED IN THE AB.

Parameter	*t-value*	DF	*p-value*
H_{max}	4.07	2	0.055
R_{max}	-0.86	2	0.481
Y'_{H2}	2.41	2	0.137

TABLE SIII. ANALYSIS OF VARIANCE OF THE GOMPERTZ AND GOMPERTZ-*TI* PARAMETERS FOR HYDROGEN PRODUCTION BY DSM155 AT DIFFERENT LIGHT INTENSITIES.

	H_{max}					R_{max}				
	DF	SS	MS	F-Value	*p*-value	DF	SS	MS	F-Value	*p*-value
Light intensity	*2*	449.8	224.9	1.10	*0.437*	*2*	2.44	1.22	9.90	0.048
Error	3	610.8	203.6			3	0.37	0.12		
Total	5	1060.6				5	2.81			

TABLE SIV. TUKEY ANALYSIS FOR R_{max} PARAMETERS OF THE GOMPERTZ AND GOMPERTZ-*TI* MODELS FOR HYDROGEN PRODUCTION BY DSM155 AT DIFFERENT LIGHT INTENSITIES.

Level comparison	Mean difference	CI (95 %)	*t*-value	*p*-value
20 klx - 10 klx	0.128	(-1.341, 1.596)	0.36	0.932
30 klx - 10 klx	1.413	(-0.055, 2.882)	4.02	0.055
30 klx - 20 klx	1.286	(-0.183, 2.754)	3.66	0.070

TABLE SV. ANALYSIS OF VARIANCE OF THE BOLTZMAN ($H_0=0$) PARAMETERS FOR HYDROGEN PRODUCTION BY DSM155 AT DIFFERENT LIGHT INTENSITIES.

	H_{max}					R_{max}				
	DF	SS	MS	F-Value	*p*-value	DF	SS	MS	F-Value	*p*-value
Light intensity	*2*	1031.7	515.8	2.83	*0.204*	*2*	1.70	0.85	5.64	0.096
Error	3	546.2	182.1			3	0.45	0.15		
Total	5	1577.9				5	2.15			

TABLE SVI. ANALYSIS OF VARIANCE OF THE Y'_{H2} IN THE HYDROGEN PRODUCTION BY DSM155 AT DIFFERENT LIGHT INTENSITITES FOT THE H_{max} PREDICTED BY GOMPERTZ AND GOMPERTZ-TI MODELS.

	H_{max}				
	DF	SS	MS	F-Value	p-value
Light intensity	2	0.32	0.16	9.12	0.053
Error	3	0.05	0.02		
Total	5	0.37			

TABLE SVII. ANALYSIS OF VARIANCE OF THE Y'_{H2} IN THE HYDROGEN PRODUCTION BY DSM155 AT DIFFERENT LIGHT INTENSITIES FOT THE H_{max} PREDICTED BY BOLTZMAN (H$_0$=0) MODEL.

	Y'_{H2}				
	DF	SS	MS	F-Value	p-value
Light intensity	2	0.30	0.151	38.65	0.007
Error	3	0.01	0.003		
Total	5	0.31			

TABLE SVIII. TUKEY ANALYSIS FOR Y'_{H2} IN THE HYDROGEN PRODUCTION BY DSM155 AT DIFFERENT LIGHT INTENSITIES FOR THE H_{max} PREDICTED BY BOLTZMAN (H_0=0) MODEL.

Level difference	Mean difference	CI (95 %)	t-value	p-value
20 klx - 10 klx	-0.4059	(-0.6672, -0.1446)	-6.49	0.015
30 klx - 10 klx	0.1182	(-0.1431, 0.3795)	1.89	0.286
30 klx - 20 klx	0.5240	(0.2627, 0.7853)	8.38	0.007

TABLE SIX. ANALYSIS OF VARIANCE OF THE $\eta_{Substrate-H2}$ IN THE HYDROGEN PRODUCTION BY DSM155 AT DIFFERENT LIGHT INTENSITIES FOR THE H_{max} PREDICTED BY GOMPERTZ AND GOMPERTZ-TI MODELS.

	$\eta_{Substrate-H2}$				
	DF	SS	MS	F-Value	p-value
Light intensity	2	4.200	2.100	1.10	0.437
Error	3	5.703	1.901		
Total	5	9.903			

TABLE SX. ANALYSIS OF VARIANCE OF THE $\eta_{Substrate-H2}$ IN THE HYDROGEN PRODUCTION BY DSM155 AT DIFFERENT LIGHT INTENSITIES FOR THE H_{max} PREDICTED BY BOLTZMAN (H_0=0) MODEL.

	$\eta_{Substrate-H2}$				
	DF	SS	MS	F-Value	p-value
Light intensity	2	13.487	6.7434	15.46	0.026
Error	3	1.308	0.4361		
Total	5	14.795			

TABLE SXI. TUKEY ANALYSIS FOR $\eta_{Substrate-H2}$ IN THE HYDROGEN PRODUCTION BY DSM155 AT DIFFERENT LIGHT INTENSITIES FOR THE H_{max} PREDICTED BY BOLTZMAN (H_0=0) MODEL.

Level comparison	Mean difference	CI (95 %)	t-value	p-value
20 klx - 10 klx	1.764	(-0.996, 4.524)	2.67	0.146
30 klx - 10 klx	3.672	(0.912, 6.431)	5.56	0.023
30 klx - 20 klx	1.907	(-0.852, 4.667)	2.89	0.123

TABLE SXII. ANALYSIS OF VARIANCE OF THE $\eta_{Light-H2}$ IN THE HYDROGEN PRODUCTION BY DSM155 AT DIFFERENT LIGHT INTENSITIES FOR THE H_{max} PREDICTED BY GOMPERTZ AND GOMPERTZ-*Ti* MODELS.

	$\eta_{Substrate-H2}$				
	DF	SS	MS	F-Value	p-value
Light intensity	2	24.15	12.07	221.07	0.001
Error	3	0.16	0.05		
Total	5	24.31			

TABLE SXIII. TUKEY ANALYSIS FOR $\eta_{Light-H2}$ IN THE HYDROGEN PRODUCTION BY DSM155 AT DIFFERENT LIGHT INTENSITIES FOR THE H_{max} PREDICTED BY GOMPERTZ AND GOMPERTZ-*Ti* MODELS.

Level comparison	Mean difference	CI (95 %)	t-value	p-value
20 klx - 10 klx	-3.304	(-4.281, -2.328)	-14.14	00.002
30 klx - 10 klx	-4.802	(-5.779, -3.825)	-20.55	0.001
30 klx - 20 klx	-1.498	(-2.474, -0.521)	-6.41	0.016

TABLE SXIV. ANALYSIS OF VARIANCE OF THE $\eta_{Light-H2}$ IN THE HYDROGEN PRODUCTION BY DSM155 AT DIFFERENT LIGHT INTENSITIES FOR THE H_{max} PREDICTED BY BOLTZMAN (H_0=0) MODEL.

	$\eta_{Light-H2}$				
	DF	SS	MS	F-Value	p-value
Light intensity	2	19.5235	9.76174	210.28	0.001
Error	3	0.1393	0.04642		
Total	5	19.6627			

TABLE SXV. TUKEY ANALYSIS FOR $\eta_{Light-H2}$ IN THE HYDROGEN PRODUCTION BY DSM155 AT DIFFERENT LIGHT INTENSITIES FOR THE H_{max} PREDICTED BY BOLTZMAN (H_0=0) MODEL.

Level comparison	Mean difference	CI (95 %)	t-value	p-value
20 klx - 10 klx	-2.989	(-3.889, -2.089)	-13.87	00.002
30 klx - 10 klx	-4.313	(-5.213, -3.412)	-20.02	0.001
30 klx - 20 klx	-1.324	(-2.224, -0.423)	-6.14	0.018

TABLE SXVI. ANALYSIS OF VARIANCE OF THE $\eta_{Light\text{-}H2}$ DETERMINED BY THE GOMPERTZ AND BOLTZMANN MODELS IN THE HYDROGEN PRODUCTION BY DSM155 AT 30 KLX.

	$\eta_{Light\text{-}H2}$				
	DF	SS	MS	F-Value	p-value
30 klx	1	0.3613	0.36132	3.94	0.185
Error	2	0.1832	0.09160		
Total	3	0.5445			

TABLE SXVII. ANALYSIS OF VARIANCE OF THE $\eta_{Light\text{-}H2}$ DETERMINED BY THE GOMPERTZ AND BOLTZMANN MODELS IN THE HYDROGEN PRODUCTION BY DSM155 AT 20 KLX.

	$\eta_{Light\text{-}H2}$				
	DF	SS	MS	F-Value	p-value
20 klx	1	0.08179	0.08179	1.63	0.330
Error	2	0.10064	0.05032		
Total	3	0.18243			

TABLE SXVIII. ANALYSIS OF VARIANCE OF THE $\eta_{Light\text{-}H2}$ DETERMINED BY THE GOMPERTZ AND BOLTZMANN MODELS IN THE HYDROGEN PRODUCTION BY DSM155 AT 10 KLX.

	$\eta_{Light\text{-}H2}$				
	DF	SS	MS	F-Value	p-value
10 klx	1	0.01251	0.012505	1.30	0.373
Error	2	0.01927	0.009635		
Total	3	0.03177			

TABLE XIX. FINAL CHARACTERISTICS OF DSM155 IN THE HYDROGEN PRODUCTION AT DIFFERENT LIGHT INTESITIES.

Light intensity (klx)	CDW (g/L)	Organic acid consumption (%)	Final pH
30	0.96	L: 60.50	7.29
		B: 96.10	
		A: 50.25	
20	1.03	L: 75.20	7.25
		B: 96.30	
		A: 62.50	
10	1.05	L: 64.70	7.50
		B: 76.90	
		A: 40.50	

Notes: A, acetate; B, butyrate; L, lactate.